Self-consistent Green's-function technique for bulk and surface impurity calculations: Surface core-level shifts by complete screening

M. Aldén, I. A. Abrikosov, and B. Johansson
Condensed Matter Theory Group, Physics Department, Uppsala University, S-75121 Uppsala, Sweden

N. M. Rosengaard and H. L. Skriver
Center for Atomic-scale Materials Physics and Physics Department, Technical University of Denmark, DK-2800 Lyngby, Denmark

(Received 8 February 1994)

We have implemented an efficient self-consistent Green's-function technique, based on the tight-binding linear-muffin-tin-orbitals method, for calculating the electronic structure and total energy of a substitutional impurity located either in the bulk or at the surface. The technique makes use of the frozen-core and atomic-sphere approximations but, in addition, includes the dipole contribution to the intersphere potential. Within the concept of complete screening, we identify the surface core-level binding-energy shift with the surface segregation energy of a core-ionized atom and use the Green's-function impurity technique in a comprehensive study of the surface core-level shifts (SCLS) of the 4*d* and 5*d* transition metals. In those cases, where observed data refer to single crystals, we obtain good agreement with experiment, whereas the calculations typically underestimate the measured shift obtained from a polycrystalline surface. Comparison is made with independent theoretical data for the surface core-level *eigenvalue* shift, and the much debated role of the so-called initial- and final-state contributions to the SCLS is discussed.

I. INTRODUCTION

During the past decade surface core-level shifts (SCLS) have become important in experimental surface science and their determination is of great value in the understanding of a wide range of surface phenomena. This includes surface electronic structure, surface structure, reconstruction, surface defects, surface energies, surface segregation, and adsorbate interaction.[1–7] Since 1978, when it was first shown that this quantity could be detected experimentally,[8] there has been considerable development in the experimental techniques.[9–20] However, due to the difficulties in resolving SCLS, the experimental work on pure elements has so far essentially been restricted to the lanthanide and the 5*d* transition series where the comparatively sharp 4*f* levels can be easily studied. It is only very recently that data for the less narrow 3*d* level of the 4*d* transition metals have been reported.[19,20]

The SCLS is tacitly defined as the difference between the *measured* core-level binding energy of a surface atom and that of the corresponding bulk atom. The theoretical interpretations of the SCLS have resulted in essentially two different models. On the one hand, from the picture that electronic relaxation following the creation of the core hole is so localized that the effect of the relaxation is independent of the geometrical environment of the excited atom, it is argued that the SCLS mainly reflects the change in the core-orbital *eigenvalue*,[1,5,12,21,22] i.e., the so-called initial-state shift.[23] On the other hand, in the approach advocated by Johansson and Mårtensson[4,6] the basic assumption is that for metals the symmetric part of the measured line profile for the core level corresponds to an electronically completely screened final state, in which the conduction electrons have attained a fully relaxed configuration in the presence of the core hole. Thereby the SCLS could be identified as the surface segregation energy of the core-ionized Z atom,[6,24,25] and as a result, SCLS have been estimated for a large number of elements in the Periodic Table by means of the $(Z+1)$ approximation (equivalent-core approximation) in conjunction with independent thermodynamical data[4,6] or tight-binding surface calculations.[26–28]

The two theoretical approaches predicted not only the correct magnitude of the SCLS,[21,22,4] but also the change of sign that was observed to occur in the middle of the 5*d* transition series.[9] By utilizing electrostatic arguments the *core-eigenvalue* shift may approximately be identified with the bulk-to-surface shift of the valence *d* band.[8] At the surface the width of the *d* band decreases and if one assumes an approximate conservation of *d* charge in each layer,[21,22,5,1] the surface *d* band must be positioned below the bulk *d* band for a *d* occupation $n_d < 5$ and above the bulk *d* band for $n_d > 5$. As a result one expects the core-eigenvalue shift to change sign in the middle of a transition series in agreement with the experimental observations. In the complete screening picture, on the other hand, the SCLS and its sign change is interpreted in terms of the change of the bonding properties due to the screening charge, relative to the original bonding of the unperturbed bulk or surface atom, respectively.[4,6] For elements with less than half-filled *d* bands the screening takes place in the bonding part of the *d* band and the total energy of the final state is lowered relative to that of the initial state as a result of the gain in valence bond en-

ergy. In contrast, the screening for the heavier elements takes place in the antibonding part of the d band and this raises the valence bond energy of the final state relative to that of the initial state. Since the screening effect is more pronounced for bulk atoms than for surface atoms due to the difference in coordination number, it follows that the SCLS should be positive in the first half of the d series and negative in the second half.

Experimental SCLS data are as yet not available for all metals, and in several cases the measurements have only been performed on polycrystalline samples. In this situation, where also the main origin of the SCLS has been under considerable debate, there is clearly a strong need for *ab initio* calculations which may serve as a guide, against which model theories and experimental uncertainties may be judged. As far as ideal and semi-infinite crystals are concerned, studies of the bulk-surface electronic structure have been performed for a large number of elemental metals by means of first-principles slab-supercell calculations. In the cases where also the accompanying core-eigenvalue shifts were reported[29–37] the general agreement between theory and available experimental single-crystal SCLS data is rather unsatisfactory.[29,36] It is generally believed that the discrepancy occurring in most cases is due to the omission of the final-state screening of the core hole.[29,31] A first-principles SCLS evaluation within the complete screening picture has previously been performed for the simple metal Al, using a five-layer slab Green's-function formalism and the $(Z+1)$ approximation for the core-ionized impurity.[38]

In this paper we present a theoretical study of SCLS for the $4d$ and $5d$ transition metals where the complete final-state screening effects are treated by calculating the electronic structure and total energy of a substitutional impurity in the form of a core-ionized atom, embedded either in the bulk or at the surface. That is, we calculate the segregation energy of a core-ionized impurity and use a Green's-function technique to treat both bulk and surface as truly infinite host systems thus avoiding the commonly used slab or supercell approximations. The method is based on the work of Andersen and co-workers[39–45] and is a straightforward extension of the tight-binding (TB) linear-muffin-tin-orbitals (LMTO) Green's-function method, implemented for surfaces and interfaces by Skriver and Rosengaard.[46] Comprehensive studies of work functions,[47] surface energies,[48,49] surface magnetism,[50] magnetic multilayer exchange interactions,[51] and stacking fault energies[52] have recently been performed by means of this technique. It has also been applied in conjunction with the coherent-potential approximation to random alloys by Abrikosov and co-workers,[53,54] and independently by Kudrnovsky *et al.*[55,56]

II. TB LMTO GREEN'S-FUNCTION METHOD FOR IMPURITIES

The calculation of a surface segregation energy is naturally divided into two different steps: (a) bulk-impurity calculation and (b) surface-impurity calculation as illustrated in Fig. 1. In the present TB LMTO Green's-function technique both host systems are treated as truly infinite without slab or supercell approximations and completely on the same level in terms of, e.g., Hamiltonian, potentials, and complex energy contour. Hence the numerical errors in the calculated impurity-solution energies are reduced to a minimum.

The present impurity technique is closely related to the work of Gunnarsson, Jepsen, and Andersen[40] and in the calculation of the Green's-function matrices we utilize the most localized, tight-binding LMTO representation.[42–44] We use the frozen-core and atomic-sphere approximations (ASA) for the potential but, in addition, include the dipole moments of the charge density in the inter-sphere Madelung potential and in the electrostatic part of the total energy. Moreover, the surface calculations are performed for ideal, geometrically unrelaxed surface layers. The validity of these approximations for the Green's-function technique may be judged from the fact that the computed surface energies[48] for most of the $4d$ series agree to better than 10% with those obtained by the full-potential, all-electron, layer-relaxed, slab-supercell method.[57]

Self-consistent electronic structure calculations for substitutional impurities in bulk systems have frequently been performed by means of the Korringa-Kohn-Rostoker (KKR) Green's-function technique.[58–61] Koenig *et al.*[62] developed a simplified KKR Green's-function method using an expansion in LMTO's. Finally, first-principles studies of impurities located in the vicinity of a surface by means of a Green's-function technique have been presented by Feibelman,[38,63] and more recently by Scheffler

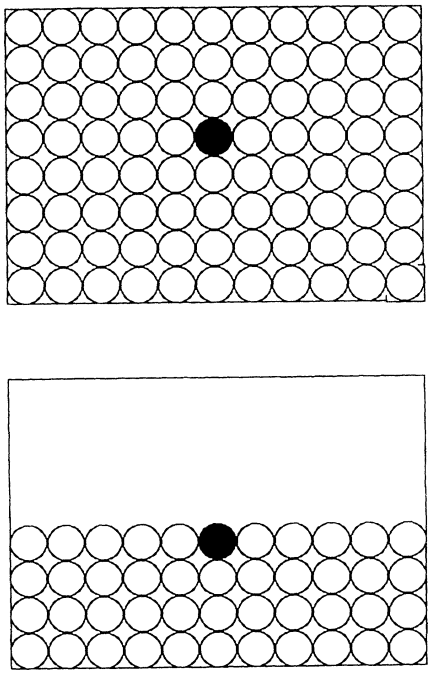

FIG. 1. Surface segregation of an impurity by means of different impurity calculations for the bulk (top) and surface (bottom).

and co-workers.[64,65]

The generalized LMTO method and the theory of transformations between MTO's in different representations are presented in depth in the papers by Andersen and co-workers.[42–44] A detailed description of the TB LMTO Green's-function technique for surfaces may be found in the works by Skriver and Rosengaard.[46,48] Here we shall restrict ourselves to the issues that are important for the bulk-surface impurity problem, with special emphasis on the construction of the Green's-function matrices, the intersphere potentials, and total energies.

A. Bulk-impurity method

In the present implementation the starting point of an impurity calculation is the Green's function for the crystalline host. This is obtained from a self-consistent band-structure calculation which yields eigenvectors $u(\mathbf{k})$ and eigenvalues $\epsilon(\mathbf{k})$ for k points in the irreducible wedge of the Brillouin zone through the eigenvalue equation

$$[H^{\gamma}(\mathbf{k}) - \epsilon\mathbf{1}]u^{\gamma}(\mathbf{k}) = 0, \tag{1}$$

where $H^{\gamma}(\mathbf{k})$ is the second-order LMTO Hamiltonian in the orthogonal (γ) representation. The Hamiltonian Green's-function matrix for the infinite crystal is then computed for complex energies z by means of the spectral representation

$$G^{\gamma}_{Q'L',QL}(\mathbf{k},z) = \sum_j \frac{u^{\gamma j}_{Q'L'}(\mathbf{k})[u^{\gamma j}_{QL}(\mathbf{k})]^*}{z-\epsilon_j(\mathbf{k})}, \tag{2}$$

where the sum runs over all band states, Q labels a site in the lattice unit cell, and L refers to combined angular momentum quantum numbers (l,m).

The KKR ASA Green's-function matrix is defined by

$$[P^{\alpha}(z) - S^{\alpha}(\mathbf{k})]g^{\alpha}(\mathbf{k},z) = \mathbf{1}\ , \tag{3}$$

where $P^{\alpha}(z)$ and $S^{\alpha}(\mathbf{k})$ are the potential functions and structure constants, respectively, within a chosen representation α. For a localized perturbation in an otherwise perfect, infinite host system it is most convenient to work in a representation that has short range. Hence we transform from the Hamiltonian Green's-function matrix to the KKR ASA Green's-function matrix in the tight-binding representation (β), by means of the expression[42]

$$g^{\beta}(\mathbf{k},z) = (\beta-\gamma)\frac{P^{\gamma}(z)}{P^{\beta}(z)} + \frac{P^{\gamma}(z)}{P^{\beta}(z)}\frac{1}{\sqrt{\dot{P}^{\gamma}(z)}} \times G^{\gamma}(\mathbf{k},z)\frac{1}{\sqrt{\dot{P}^{\gamma}(z)}}\frac{P^{\gamma}(z)}{P^{\beta}(z)}\ , \tag{4}$$

which only involves (l,l')- and energy-dependent scalings. For the potential functions and their energy derivative, we employ the second-order expressions given elsewhere.[42,44,46]

The calculation of the structural host Green's-function matrix which enters the Dyson equation below involves a time-consuming k-point integration over the whole Brillouin zone (BZ), i.e.,

$$g^0_{R'L',RL}(z) = \int_{\mathrm{BZ}} g^{\beta}_{Q'L',QL}(\mathbf{k},z)e^{-i\mathbf{k}\cdot(\mathbf{T}-\mathbf{T}')}d^3k. \tag{5}$$

Here R denotes lattice sites in a chosen cluster, centered around the impurity, in which potentials and charge densities will be allowed to relax self-consistently and T is a primitive translation vector for which $\mathbf{R} = \mathbf{T}+\mathbf{Q}$. As pointed out by several workers,[66,62,53] the integral in Eq. (5) may be reduced to the irreducible BZ (IBZ) due to the transformation properties of the KKR ASA Green's-function matrix. It transforms as the product of two harmonics of the kind used in the calculation of the structure constants. Hence, in the case of no Q dependence, i.e., one-atomic-unit cells,

$$g^{\beta}(\Gamma\mathbf{k},z) = Ug^{\beta}(\mathbf{k},z)U^{-1}, \tag{6}$$

where U is the unitary transformation matrix for the symmetry operator Γ of the point group. For a more general case valid for pure elemental crystals in the fcc, bcc, or hcp phases, i.e., those which are considered in this work, Eq. (5) becomes equivalent to[62]

$$g^0_{R',R}(z) = \int_{\mathrm{IBZ}} e^{i\mathbf{k}\cdot(\mathbf{Q}-\mathbf{Q}')}\sum_j U_j g^{\beta}_{Q',Q}(\mathbf{k},z) \times U_j^{-1}e^{-i\Gamma_j\mathbf{k}\cdot(\mathbf{R}-\mathbf{R}')}d^3k, \tag{7}$$

where the sum runs over the elements j of the point group. However, even if g^0 is constructed using (7) instead of (5), the computational effort grows quickly with cluster size due to the phase factors appearing in these expressions. Following Gonis *et al.*,[66] for each (Q',Q) pair we therefore only calculate g^0 for a minimal set of "inequivalent" (R,R') blocks, which do not transform to one another by a symmetry operation. Hence, if Γ_m is a symmetry operator represented by U_m and

$$\Delta(\mathbf{R})_{ij} = \Gamma_m\Delta(\mathbf{R})_{kl}\ , \tag{8}$$

where $\mathbf{R}_i - \mathbf{R}_j \equiv \Delta(\mathbf{R})_{ij}$ then, in analogy to (6), it is easily verified that

$$g^0_{R_k,R_l;Q'Q}(z) = U_m g^0_{R_i,R_j;Q'Q}(z)U_m^{-1}. \tag{9}$$

It turns out that for an impurity-centered cluster with 2 shells in the fcc crystal [13 atoms, 169 (R,R') blocks] only 5 blocks need to be calculated using Eq. (7), and with 7 shells [87 atoms, 7569 (R,R') blocks] this number becomes 26.

If lattice relaxations are neglected a perturbation from the perfect host system is described in LMTO ASA theory solely by the potential functions. Hence the change in atomic species at the impurity site and the relaxation of the potentials on the neighboring sites is taken into account by

$$\Delta P_{RL}(z) = P_{RL}(z) - P^{\mathrm{host}}_{QL}(z) \tag{10}$$

and the finite Dyson equation

$$g(z) + g^0(z)\Delta P(z)g(z) = g^0(z), \tag{11}$$

giving the structural Green's-function matrix g for the imperfect crystal. Again, the computational efforts grow quickly with cluster size since the matrices here scale with the number of perturbed sites. Following Slater[67] and others,[40,59,68] we therefore transform g^0 from the previously used site and cubic harmonic representation to the symmetry representation, by means of the unitary transformation

$$g^{0;\lambda\alpha}_{\mu\mu'}(z) = \sum_{ss'} \sum_{\substack{R \in s \\ R' \in s'}} \sum_{lm,l'm'} S^{\lambda\alpha;\mu}_{Rlm} g^0_{Rlm,R'l'm'}(z) S^{\lambda\alpha;\mu'}_{R'l'm'}, \tag{12}$$

where the symmetrization matrices S are calculated according to the scheme given by Ries and Winter.[69] The first sum in (12) runs over shells s and the index μ denotes the basis function belonging to a particular column α of the representation λ. In the symmetry representation the Dyson equation is block diagonalized and

$$g^{\lambda\alpha}(z) + g^{0;\lambda\alpha}(z)\Delta P(z) g^{\lambda\alpha}(z) = g^{0;\lambda\alpha}(z) \tag{13}$$

may instead be solved separately for each (λ, α) set. It is (13) that, together with the Poisson and scalar-relativistic Dirac equations,[46] is solved in typically 10–15 iterations until self-consistency is achieved in charge densities and potentials. Convergence speed benefits from the use of linear-response theory, in a manner analogous to the prescription given by Skriver and Rosengaard.[48] To obtain the linear-response matrix and the site projected state densities, one needs a partial backtransformation to the nonsymmetrized Green's-function matrix g, inverse to (12), at each iteration step. However, the computational cost of performing the backtransformation is small compared to the gain achieved by block diagonalizing the Dyson equation.

B. Surface-impurity method

At the outset of an impurity calculation for a surface, one needs the surface Green's-function $g^s(\mathbf{k}_\parallel, z)$ of the host, sampled on a complex energy contour and on $k_\parallel$ points in the irreducible part of the two-dimensional (2D) Brillouin zone (I2BZ). In addition, one needs potential functions, the electrostatic intersphere potential, and total energies, as well as appropriate starting charge densities, corresponding to the real surface. These quantities are generated by a self-consistent surface calculation for the host material, using the most recent version of the TB LMTO Green's-function technique for surfaces and interfaces.[46,48] In the present implementation the 2D layer representation of the underlying bulk-vacuum Green's-function is obtained by means of the principal layer technique by Wenzien *et al.*,[70] avoiding k-point integration in the direction perpendicular to the surface.

We obtain the cluster Green's-function matrix analogous to (7), i.e.,

$$g^0_{R',R}(z) = \int_{\text{I2BZ}} e^{i\mathbf{k}_\parallel \cdot (\mathbf{Q}_\parallel - \mathbf{Q}'_\parallel)} \sum_j U_j g^s_{Q,Q'}(\mathbf{k}_\parallel, z) \times U_j^{-1} e^{-i\Gamma_j \mathbf{k}_\parallel \cdot (\mathbf{R}_\parallel - \mathbf{R}'_\parallel)} d^2k, \tag{14}$$

where Q here belongs to the layered 2D unit cell $\mathbf{Q} = (\mathbf{Q}_\parallel, Q_\perp)$ and $\mathbf{R} = (\mathbf{R}_\parallel, R_\perp)$ is a lattice vector of the cluster centered around the impurity site. The rotation matrices U_j here correspond to symmetry operations Γ_j which belong to the common subset of the surface and bulk symmetry groups.

The rest of the formalism follows directly from the 2D analogy to Eqs. (8)–(13). Hence, for the application of (8) and (9), $R_\parallel$ is substituted for R, and in the symmetry transformation (12) the first sum runs over "rings" instead of shells, the site-equivalency being determined by symmetry transformations. The Dyson equation (13) is block diagonalized into irreducible representations corresponding to the point groups C_{3v} for the fcc(111) and hcp(0001) surfaces, C_{2v} for the bcc(110) surface, and C_{4v} for the fcc(100) surface. Finally, ΔP in the Dyson equation represents the deviation of the potential functions from those of the unperturbed surface.

C. The intersphere potential

The intersphere contribution V_I to the one-electron potential stems from the long-range electrostatic interactions present in the system. In a conventional bulk calculation within the ASA, these are accounted for by a Madelung potential alone, i.e., an infinite sum of charge density monopoles. However, at a surface it is important to include the dipole terms in the multipole expansion[46] and we shall do so in the present work.

For the impurity problem it is convenient to work with the induced changes in the valence monopoles q (net charges) and dipoles $\mathbf{p}$

$$\Delta q_R = q_R - q_R^{\text{host}}, \quad \Delta \mathbf{p}_R = \mathbf{p}_R - \mathbf{p}_R^{\text{host}} \tag{15}$$

at each site R relative to those of the unperturbed host system. The definitions of q and $\mathbf{p}$ may be found in Ref. 46. In the presence of an impurity the intersphere potential at site R may be written

$$V_{I;R} = V_{0;R} + \Delta V_{s;R} + \Delta V_{p;R} + \Delta V_{\text{out};R} \tag{16}$$

where $V_{0;R}$ is the intersphere potential in the unperturbed host system and $\Delta V_{\text{out};R}$, to be defined below, is a term which acts to maintain the original charge $q^{\text{host}}_{\text{total}}$ of the unperturbed cluster. For the bulk geometries used here $q^{\text{host}}_{\text{total}}$ is always zero, but for a cluster centered in the surface layer it becomes of the order of one electron. Finally, $\Delta V_{s;R}$ and $\Delta V_{p;R}$ are the deviations from the original monopole and dipole contributions, respectively. These are given by

$$\Delta V_{s;R} = 2 \sum_{R' \neq R} \frac{\Delta q_{R'}}{|\mathbf{R} - \mathbf{R}'|}, \tag{17}$$

$$\Delta V_{p;R} = 2\sqrt{3} \sum_{R' \neq R} \frac{\Delta \mathbf{p}_{R'} \cdot (\mathbf{R} - \mathbf{R}')}{|\mathbf{R} - \mathbf{R}'|^3}, \tag{18}$$

where the sums run over the perturbed sites that are included in the cluster. For consistency, ΔV_p is included in V_I also for the bulk impurity calculation, although here the dipole moments are rather small. Finally, the excess charge in the perturbed region

$$\Delta q_{\text{total}} = \sum_{R'} \Delta q_{R'} \tag{19}$$

is typically 10^{-3}–10^{-2} electrons and is distributed uniformly over the N_{out} sites in the first two shells outside the cluster. This then forms an additional monopole contribution

$$\Delta V_{\text{out};R} = 2 \sum_{R_{\text{out}}}^{N_{\text{out}}} \frac{-\Delta q_{\text{total}}}{N_{\text{out}} |\mathbf{R} - \mathbf{R}_{\text{out}}|} \tag{20}$$

to the intersphere potential $V_{I;R}$ and maintains the charge neutrality of the complete system.

D. The solution energy

In the Born-Oppenheimer, the local-density, the atomic-sphere, and the frozen-core approximations, the total valence-electron energy E may be calculated according to the prescription given in Ref. 46. Furthermore, within the ASA the total energy E including the electrostatic contributions may be partitioned into atomic-sphere-dependent terms E_R, i.e.,

$$E = \sum_R E_R \ , \tag{21}$$

where the sum runs over sites in a cluster or in a unit cell. For the electrostatic contribution to E_R we have

$$E_{\text{stat};R} = E^0_{\text{stat};R} + (V_{0;R} + \tfrac{1}{2}\Delta V_{s;R})\Delta q_R + \Delta V_{p;R} q_R, \tag{22}$$

where $E^0_{\text{stat};R}$ refers to the unperturbed system, the factor $1/2$ is introduced to correct for double counting, and q_R is the total charge at site R. For a sufficiently large cluster the contribution due to ΔV_{out} becomes very small and is safely neglected in Eq. (22) for the present applications.

In the underlying surface calculation for the host material, the surface energy E_S is calculated as the sum

$$E_S = \sum_Q E_{S,Q} \tag{23}$$

over the surface region of the difference[46,48]

$$E_{S,Q} = E^{\text{2D}}_Q - E^{\text{3D}}_Q \tag{24}$$

between the total energy E^{2D}_Q obtained in the surface calculation and projected onto the atomic sphere at site Q in the surface region and the corresponding energy E^{3D}_Q obtained in the bulk calculation.

The solution energy of a substitutional impurity in the bulk may be expressed as[60]

$$E^{\text{sol}}_{\text{bulk}} = E_{Q_b} + \sum_{R \neq Q_b} (E_R - E^{\text{3D}}_R) - E^{\text{imp}}, \tag{25}$$

where E_{Q_b} is the atomic-sphere projected total energy of the impurity atom located at site Q_b in the host environment and E^{imp} is the total energy per atom of bulk impurity species. The sum in Eq. (25) runs over the rest of the sites in the cluster, incorporating the induced changes of the total energy of the host atoms due to the presence of the impurity. Similarly, the solution energy of a substitutional impurity located at the site Q_s in the surface region may be expressed as

$$E^{\text{sol}}_{\text{surf}} = E_{Q_s} + \sum_{R \neq Q_s} (E_R - E^{\text{2D}}_R) - E^{\text{imp}}, \tag{26}$$

where the sum runs over host and vacuum atomic spheres centered around the impurity site.

In the presence of a localized defect the induced changes in the one-electron energies are sensitive to violations of the Friedel sum rule. If these changes $\Delta E^{\text{one-el}}$ are extracted through a local summation at each site, this causes a slow convergence in the total energies with respect to cluster size.[60] We therefore employ the less sensitive formula[40]

$$\Delta E^{\text{one-el}} = \epsilon_F \Delta n - \frac{1}{i\pi} \oint \eta(z) dz \ , \tag{27}$$

which refers to the whole crystal but may be projected onto a particular site by taking $\Delta E^{\text{one-el}}_R = \Delta E^{\text{one-el}}/N_c$, where N_c is the cluster size. In (27), Δn is the total valency change and the generalized phase shift $\eta(z)$ may be obtained from

$$\eta(z) = \ln\left(\det\{G^{0;\gamma}(z)[G^{\gamma}(z)]^{-1}\}\right), \tag{28}$$

where $G^{0;\gamma}(z)$ is the unrelaxed and $G^{\gamma}(z)$ the relaxed Hamiltonian Green's-function matrices in the γ representation and branch cuts in the logarithm are avoided by choosing the phase continuous on the complex energy contour, on which the integral in Eq. (27) is evaluated.[71]

E. SCLS and segregation energy

To calculate core-level binding energies Johansson and Mårtensson[4] introduced a Born-Haber cycle which connected the initial and final states of the core ionization process and used it to study the shift of the core-level binding energy between bulk and free atoms. When the cycle is applied to the shift in core-level binding energy between bulk (b) and surface (s) atoms one obtains the expression

$$\Delta^{bs} = [E^{Z^*,s}_{\text{coh}} + E^{Z^*,s}_{\text{imp}}(Z) - E^{Z,s}_{\text{coh}}] - [E^{Z^*,b}_{\text{coh}} + E^{Z^*,b}_{\text{imp}}(Z) - E^{Z,b}_{\text{coh}}] \tag{29}$$

in terms of the solution energies $E_{\rm imp}$ of the core ionized Z^* atom in the Z bulk or Z surface and the corresponding cohesive energies $E_{\rm coh}$. When written in this form the first and the second set of square brackets in (29) represent the energies necessary to replace a Z atom by a Z^* atom at the surface and in the bulk, respectively, and their difference is the energy of surface segregation of a Z^* atom in a Z host.

Unfortunately, none of the terms involved, except the cohesive energy, can be obtained experimentally. Neither could these terms, at the time the Born-Haber cycle was introduced, be calculated from first principles. To connect the surface core-level shift to measurable quantities one therefore introduced the equivalent core approximation where a Z atom with a deep core hole is represented by the element of nuclear charge $Z+1$. Thereby the surface core-level shift may be identified as the heat of surface segregation of a $Z+1$ atom in a Z metal, which in favorable cases may be estimated from alloy studies.

A different estimate of the surface core-level shift may be obtained if one regards the surface energy E_S as the difference in cohesive energy between surface and bulk atoms. In that case (29) may be written[6,24]

$$\Delta_c^{bs} = (E_S^{Z+1} - E_S^Z) + [E_{\rm imp}^{Z+1,s}(Z) - E_{\rm imp}^{Z+1,b}(Z)], \quad (30)$$

and this form has the advantage that it separates the contributions to the SCLS into two distinct parts: (a) a surface energy difference, which especially for transition metals is usually thought of as the dominant contribution, and (b) an impurity contribution, which may be defined simply as the remaining "cross term" needed to identify (30) with the surface segregation energy of a $(Z+1)$ impurity in the Z metal host.[6] If the impurity aspect may be neglected Eq. (30) simply becomes

$$\Delta_c^{bs} \approx E_S^{Z+1} - E_S^Z \quad (31)$$

in which case the equation may be used to estimate the surface core-level shift and the related segregation energy from known surface energies. From the parabolic behavior of the surface energy through the $4d$ and $5d$ series, it becomes immediately obvious that Δ_c^{bs} changes sign in the middle of the series.

With the recent advance in computational techniques the surface segregation energy may be obtained directly from first principles and there is no need for the equivalent core approximation. Moreover, the complete separation in Eq. (30) of the SCLS into surface energy- and impurity-dependent parts becomes somewhat superficial on the basis of the present techniques, where the segregation energy is obtained directly from two different impurity calculations. In particular, one should not try to identify the impurity term $E_{\rm imp}^{Z+1,s}(Z)$ above with the solution energy $E_{\rm surf}^{\rm sol}$ in Eq. (26), since the former already contains terms related to the surface energy itself.

In a slab or a supercell approach the surface segregation energy, defined as the energy required to interchange an impurity atom in the bulk with a host atom at a particular surface site Q_s, may be calculated as the difference between the total energy of a system consisting of unperturbed bulk plus surface with impurity and the total energy of a system containing a pure surface plus bulk with impurity. However, in the present case it is more convenient to obtain the segregation energy in terms of the impurity solution energies defined in (25) and (26). If we write down the expression for the total energy of the two systems mentioned above and make use of the atomic-sphere projection, we find

$$E_{\rm segr}^{\rm imp} = E_{\rm surf}^{\rm sol} - E_{\rm bulk}^{\rm sol} - E_{S,Q_s}, \quad (32)$$

where the last term is defined in (24). This contribution represents the Q_s-projected surface energy of the host and accounts in the ASA for the transfer of a host atom from the surface site Q_s to a bulk site which is an integral part of the segregation process. One should note that the original total energy of the impurity species $E^{\rm imp}$ is included in the two impurity solution energies (25) and (26) and therefore is canceled in the expression for the segregation energy (32). Hence the condition under which $E^{\rm imp}$ is calculated is irrelevant for the segregation energy.

In the frozen-core approximation a neutral core-ionized host atom may be created in a self-consistent atomic calculation where the electron in the chosen core level is transferred into an extra valence state, and the surface core-level shift may then be obtained from (32) as the segregation energy of this Z^* impurity, i.e.

$$\Delta_c^{bs} = E_{\rm segr}^{Z^*}. \quad (33)$$

The complete procedure may be described as two impurity calculations where the first involves a TB LMTO bulk calculation, the construction of the Green's-function matrix for the structural host, and a self-consistent bulk-impurity calculation which gives the solution energy of the core-ionized host atom $E_{\rm bulk}^{{\rm sol};Z^*}$. The second step involves a TB LMTO surface calculation,[46,48] which gives the atomic-sphere partitioned total and surface energies, the construction of the structural host Green's-function matrix corresponding to the real surface, and a self-consistent surface-impurity calculation, which yields the solution energy of the surface impurity $E_{\rm surf}^{{\rm sol};Z^*}$. Finally, all the results are combined to give the SCLS in the form of the surface segregation energy of the core-ionized host atom.

F. Details of the calculations

The parameters that must be chosen at the outset of an impurity calculation by the present technique are the cluster size, the density of k points, the complex energy sampling, and the form of the exchange-correlation potential. We apply the (minimal) *spd* basis set that has been used in the previous study of the surface energies of metals.[48] For the bulk k-space integration in (7) we use 1785 points in the irreducible wedge of the Brillouin zone for the bcc structure, 1505 points for the fcc structure, and 1500 points for the hcp structure. For the surface $k_\parallel$ integration in (14) we use 256 special points in the irreducible part of the two-dimensional Brillouin zone for the bcc(110) surface, 136 points for the fcc (100) surface, and

252 points for the fcc(111) and hcp(0001) surfaces. The moments of the state density are calculated by integrating the Green's function on a complex energy contour, using a Gaussian integration technique with 16 points distributed exponentially on a semicircle enclosing the occupied states. Finally, exchange and correlation were included in the parametrization of the local density approximation given by Vosko *et al.*[72]

Based on tests of the convergence of the total energy, utilizing the generalized phase shift for the one-electron energies, we use a cluster region consisting of 51 atoms for the bcc crystal, 55 for the fcc crystal, and 51 for the hcp crystal. In the fcc and bcc crystals this corresponds to one impurity site plus four shells of nearest neighbor host atoms and in the hcp crystal to one impurity site plus eight shells of host atoms. If the generalized phase shift is replaced by a local summation of one-electron energies, we have found that $\sim$ 150 atoms are required for shell convergency. Finally, in the surface calculations we use a surface region consisting of four layers of metal plus two layers of empty spheres simulating the vacuum.

III. RESULTS

In the following we shall present the surface core-level shifts of the $4d$ and $5d$ transition metals as calculated by the procedure described in the preceding section assuming for each metal the fcc, bcc, and hcp crystal structures. The core hole to be screened is taken as a $4f$ level in the $5d$ series and a $3d$ level in the $4d$ series since these are the levels measured in experiment. All calculations are performed at the experimentally observed equilibrium volumes and at the experimentally observed c/a ratios for the hcp elements.

A. 5d transition metals

The SCLS of the fcc(111) surfaces of the $5d$ elements from Yb to Pt are presented in Fig. 2 together with available experimental data. It is seen that for the elements Lu – Ir the calculated SCLS decreases almost linearly with d-band filling in qualitative agreement with the previous tight-binding studies.[22,26] It is also seen that calculated SCLS exhibits a change of sign between W and Re corresponding to an initial-state d occupancy of $\sim$4.5. The linear behavior and the sign change may be explained within the simple picture of d-electron contribution to the surface energy, suggested by Friedel.[73] According to this picture the surface energy exhibits a parabolic variation with the d-band occupation and if we write the approximate relation (31) in the form

$$\Delta_c^{bs} \approx \frac{dE_S^Z}{dZ}, \tag{34}$$

it follows immediately that the surface core-level shift should decrease linearly across the series and exhibit a sign change when the d band is half full.

Within the complete screening picture the variation of the SCLS is related to the properties of the screening electrons. In Fig. 3 we have therefore plotted the d screening charge, defined as the d occupation on the impurity site after the core ionization minus the d occupation of the site before the ionization. It is seen that except for Yb and Pt the screening charge is close to one electron, both in the bulk and at the surface. Hence the SCLS is expected to vary smoothly through the series except at the

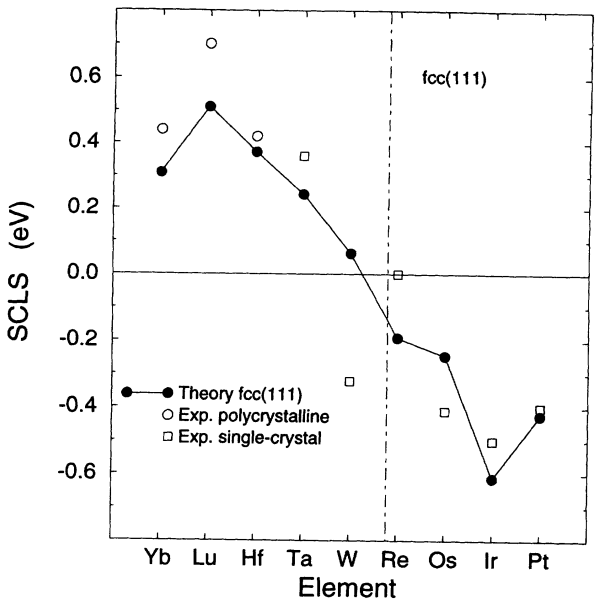

FIG. 2. The calculated surface core-level shift for the fcc(111) surfaces of the $5d$ metals (solid circles). These are compared to experimental data obtained from the most closely packed surface of the correct structures (open squares) or from polycrystalline samples (open circles). The vertical dashed line marks a half-filled d band (initial state).

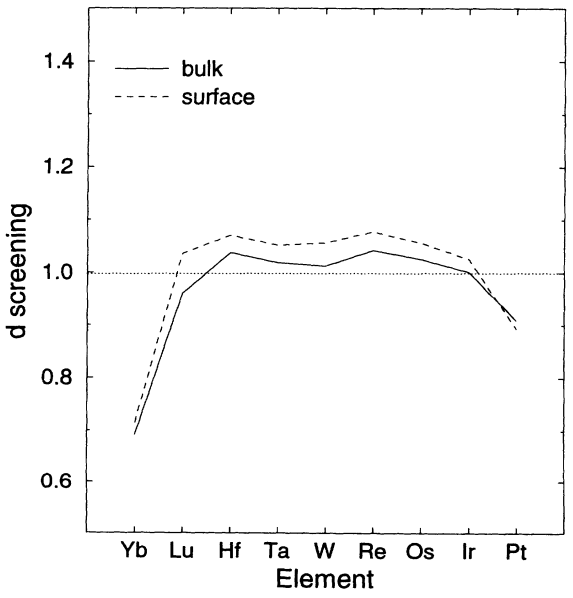

FIG. 3. Calculated d screening charge on the core-ionized atom for the fcc(111) surfaces of the $5d$ metals. The horizontal dotted line marks the value 1 as a guide to the eye.

two ends where the less efficient d screening may partially explain the reduced magnitude of the SCLS in Yb and Pt shown in Fig. 2.

The prominent features present in the measured SCLS are clearly not reproduced when the calculations are restricted to the fcc(111) face alone. SCLS calculated for the experimentally observed crystal structures give a substantially modified behavior across the series, as shown in Fig. 4. First, the sign change now occurs between Ta and W, in agreement with the experimental observation by van der Veen *et al.*[9] and with recent tight-binding studies.[28] Second, the anomalous values of the measured SCLS for W(110) (Ref. 16) and Re(0001) (Ref. 14) as well as the values for Os(0001) (Ref. 14) and Pt(111) (Refs. 11 and 7) are fully reproduced by the calculations. The discrepancy for Ta(110) may be traced to the fact that the ASA underestimate the surface energy in Ta (Ref. 48) and hence according to (31) overestimate the corresponding SCLS. A similar effect, but smaller and of opposite sign, may be suspected for Ir(111).

For the elements Yb(111), Lu(0001), and Hf(0001) the theoretical values in Fig. 4 are systematically lower than the measured shifts. This disagreement may be attributed to the fact that the experimental values[17,18] here refer to polycrystalline samples, since in general the magnitude of the SCLS should be smallest for the most closely packed surface structure. Also, recent experimental investigations[74] on lanthanide metals have produced shifts which are considerably smaller than older data, apparently due to improved measurements and higher quality samples. To investigate the cause of the discrepancy we performed calculations for Yb-Hf also for the more open (100) face of the fcc crystal. In Yb and Hf this raises the shifts closer to the observed values, as listed in Table I. Much to our surprise, however, for Lu the fcc(100) shift is lower than both the hcp(0001) and the fcc(111) shifts. This unexpected behavior signals a sensitivity of the screening to the actual state densities involved, i.e., beside the general dependence on the "uniform" surface band narrowing. The calculated state densities presented in Fig. 5 for hcp(0001) and fcc(100) Lu represent the *initial state* of the valence configuration, thus giving only part of the information needed in a complete analysis. One may speculate, however, that the strong surface resonance found close to the Fermi level in the fcc(100) face is responsible for the anomalous low SCLS.

A systematic investigation of the dependence of the SCLS on the crystal structure through the $5d$ series is presented in Fig. 6. Here the calculations were performed for the most closely packed surface of the fcc, bcc, and hcp structures of each element. It is seen that except for Re, the SCLS in the hcp and fcc structures are very similar and smoothly varying through the series, which may be attributed to the fact that the state density of the two phases is rather uniform. This makes the parabolic variation of the surface energy with occupation number a good approximation and an almost linear behavior follows from (34). In contrast, the bcc SCLS vary dramatically across the series in a manner which appears to be related to the well-known double hump of the bcc state density.

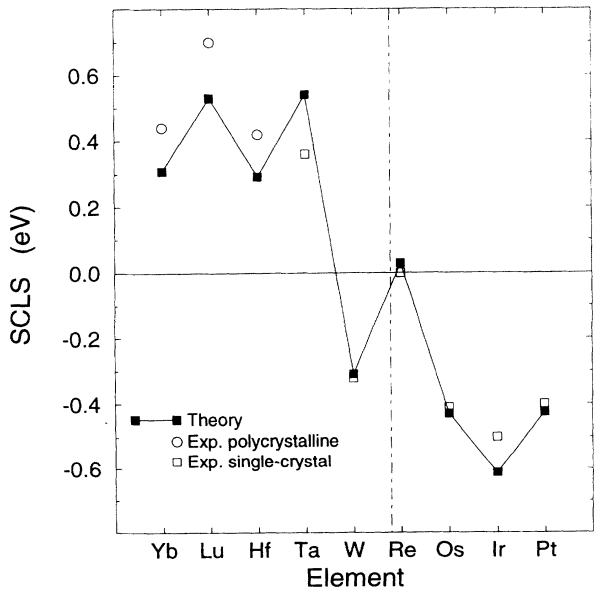

FIG. 4. The calculated surface core-level shift of the $5d$ metals for the most closely packed surface of the experimentally observed crystal structures (solid squares), compared to experimental data for the same structure (open squares) or to that of polycrystalline samples (open circles). The vertical dashed line marks a half-filled d band (initial-state).

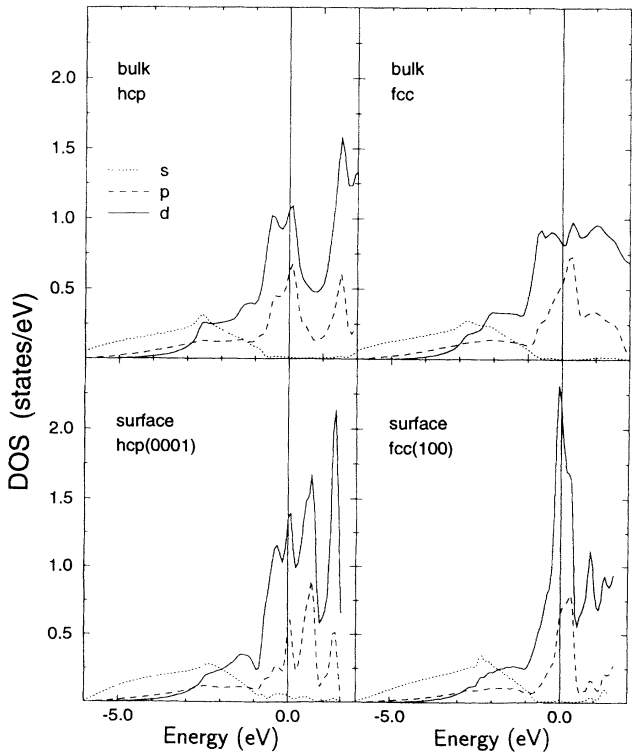

FIG. 5. Calculated s, p, and d state densities (DOS) for Lu; hcp(0001) (left) and hypothetical fcc(100) (right); bulk (top) and surface layer (bottom).

The rapid variation of the SCLS in the bcc phase may be explained in terms of the screening properties. Within the complete screening picture, the SCLS of a system with n d electrons in the initial state in the bulk and at the surface may be related to the d state density by means of the relation

$$\Delta_c^n \approx -(C_{\tilde{n}}^S - C_{\tilde{n}}^B) , \tag{35}$$

to be derived in Sec. IV A. In (35) $C_{\tilde{n}}^{S,B}$ is the d-band centroid for the bulk (B) and surface (S), respectively, corresponding to a d occupation of $\tilde{n} \approx n + 1/2$. Since by definition

$$\tilde{n} - 5 = \int_{C_{\tilde{n}}}^{\epsilon_F} D(\varepsilon)d\varepsilon = (\epsilon_F - C_{\tilde{n}})\tilde{D}, \tag{36}$$

$D(\varepsilon)$ being the local d state density and $\tilde{D}$ its average over the interval, one obtains, for the qualitative variation of the SCLS,

$$\partial\Delta_c/\partial n \sim -(1/\tilde{D}^B - 1/\tilde{D}^S). \tag{37}$$

Hence for the bcc structure with its well-known two-peaked d state density the low (bulk) density in the middle of the series gives rise to the steep descent observed in the full calculations in Fig. 6.

If we simulate the fcc phase by a constant state density, where the bandwidth at the surface is reduced by δW, the SCLS will follow the linear relation[28]

$$\Delta_c \sim (1/2 - \tilde{n}/10)\delta W. \tag{38}$$

With δ=0.20, i.e., a 20% reduction of the bandwidth at

TABLE I. Calculated (Calc.) and observed (Expt.) surface core-level shifts of the 5d (left) and 4d (right) transition metals. Polycrystalline experimental data are given in parentheses.

	5d metals			4d metals		
Crystal (surface)	Element	SCLS (eV)		Element	SCLS (eV)	
		Calc.	Expt.		Calc.	Expt.
fcc (111)	Yb	0.311	(0.44)[a]	Sr	0.195	
fcc (100)		0.451				
bcc (110)		0.254				
hcp (0001)	Lu	0.530	(0.70)[b]	Y	0.409	0.7–0.9[g]
fcc (111)		0.512			0.396	
fcc (100)		0.394				
bcc (110)		0.333				
hcp (0001)	Hf	0.292	(0.42)[b]	Zr	0.226	
fcc (111)		0.372			0.279	
fcc (100)		0.450				
bcc (110)		0.377				
bcc (110)	Ta	0.541	0.360[c]	Nb	0.466	
fcc (111)		0.242			0.097	
hcp (0001)		0.184				
bcc (110)	W	−0.309	−0.321[d]	Mo	−0.316	−0.330[h]
fcc (111)		0.063			−0.008	
hcp (0001)		0.099				
hcp (0001)	Re	0.030	0.00[e]	Tc	−0.027	
fcc (111)		−0.191			−0.207	
bcc (110)		−0.486				
hcp (0001)	Os	−0.430	−0.41[e]	Ru	−0.444	
fcc (111)		−0.245			−0.312	
bcc (110)		−0.344				
fcc (111)	Ir	−0.612	−0.50[b]	Rh	−0.593	
hcp (0001)		−0.662				
bcc (110)		−0.162				
fcc (111)	Pt	−0.423	−0.40[f]	Pd	−0.232	−0.2[h]
hcp (0001)		−0.444				
bcc (110)		−0.240				

[a]Mårtensson (Ref. 18).
[b]Flodström *et al.* (Ref. 17 and references therein).
[c]Riffe and Wertheim (Ref. 16).
[d]Riffe *et al.* (Ref. 15).
[e]Mårtensson *et al.* (Ref. 14).
[f]Baetzold *et al.* (Ref. 11) and Tillborg (Ref. 7).
[g]Barrett *et al.* (Ref. 13).
[h]Lundgren *et al.* (Ref. 19).

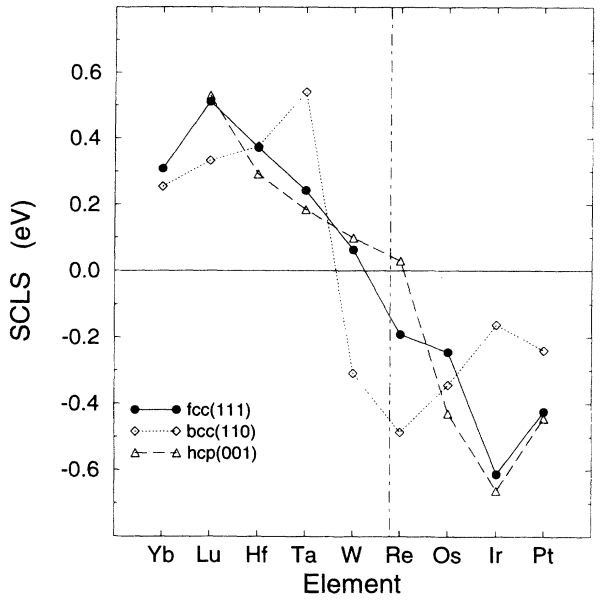

FIG. 6. Comparison between calculated surface core-level shifts of the 5*d* metals for the most closely packed surface of the fcc (circles), hcp (triangles), and bcc (diamonds) crystal structures. The vertical, dashed line marks a half-filled *d* band (initial state).

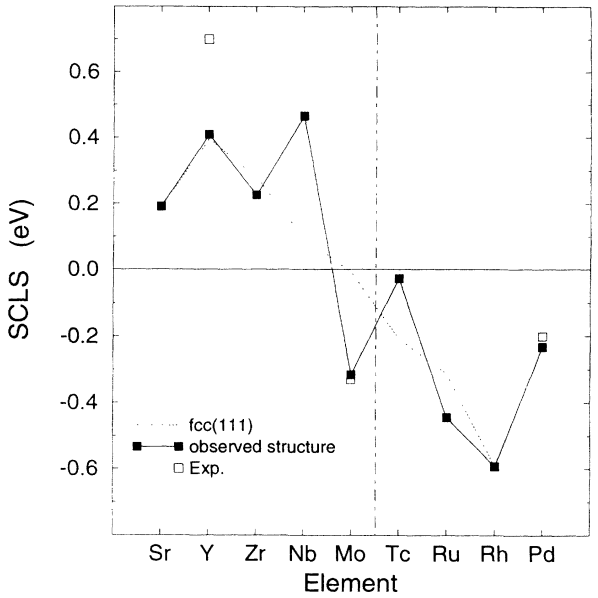

FIG. 7. The calculated surface core-level shift of the 4*d* metals for the most closely packed surface of the experimentally observed crystal structures (solid squares) and for the (111) surface of the fcc crystal. Experimental single-crystal data are denoted by open squares. The vertical dashed line marks a half-filled *d* band (initial-state).

the surface, and $W \approx 5$ eV, the shift varies from about +0.5 eV to −0.5 eV through the series. This simple estimate is in astonishing agreement with the results obtained in the full fcc(111) calculations shown in Fig. 2.

B. 4*d* transition metals

The SCLS for the 4*d* transition metals are displayed in Fig. 7 where we show the calculated shifts of the fcc(111) faces and of the most closely packed surfaces of the observed crystal structures, together with the known experimental data for Y(0001),[13] Mo(110), and Pd(111).[19] It is seen that the trend across the 4*d* series essentially follows that of the 5*d* series. For Mo(110) and Pd(111) the calculated SCLS are in very good agreement with experiment, in analogy to, e.g., W(110) and Pt(111). To our knowledge no experimental data for, e.g., Tc(0001), exist. The calculations predict that the SCLS will vary smoothly across the series except for Mo(110) and Tc(0001) where a rapid variation is expected. This is similar to the 5*d* case and due to the dependence on crystal structure. In Y(0001) we find a discrepancy of 0.3 eV between theory and experiment which is difficult to understand even on a qualitative basis. The theoretical and experimental results for the 4*d* metals are summarized in Table I parallel to the corresponding data for the 5*d* metals.

IV. DISCUSSION

With the present results there exist theoretically determined SCLSs for the 4*d* and 5*d* transition metals, obtained completely from first principles within the final-state screening picture. The agreement with single-crystal measurements, which is experienced in most cases, lends strong support to the theoretical approach used to obtain the SCLS and suggests that the assumption of complete final-state screening is indeed valid for metallic systems. A main issue in previous theories and interpretations of the SCLS, however, has been the relative importance of the so-called initial-state and final-state contributions to the shift. It is therefore appropriate in the present context to review the basic concepts involved[1,2] and, with the aid of new information, shed extra light on this controversial subject.

It is well known that the shape of an x-ray core-level spectrum contains several contributions, namely, the so-called shakeup and shakeoff intensities towards higher binding energies relative to that of the main peak (MP). The removal of the photoelectron is much faster (10^{-17} s) than the relaxation process (10^{-15} s) of the valence electrons,[7] and there is essentially no time for redistribution of the valence levels during the photoemission event. However, the total wave function $\Psi_{\rm ph}$ may be expressed as the linear combination

$$\Psi_{\rm ph} = \sum_i \langle \psi_i | \Psi_{\rm ph} \rangle \psi_i \tag{39}$$

of eigenfunctions ψ_i of the Hamiltonian which represents the system with a missing core electron.[75] The spectral features convolute the corresponding eigenvalues ϵ_i. The central assumption on which the present impurity calculations are based, and which is used by Johansson and Mårtensson,[4,6] is that the MP, i.e., the symmetric part of the line profile, corresponds to the ground state ψ_0.[76]

The difference between the ground-state energy ϵ_0 and the spectral weight of the various intensities may be used as a measure of the electronic relaxation energy. Hence the difference in relaxation energy for a surface atom relative to a bulk atom is commonly identified with final-state effects in the SCLS.

A. The initial- and final-state contributions to the SCLS

The SCLS Δ_c is the difference between two binding energies of a core-level X belonging to a bulk or a surface atom, i.e., the difference between two total energy differences

$$\begin{aligned}\Delta_c &= E_{N-1}(X_{\rm surf}) - E_N - [E_{N-1}(X_{\rm bulk}) - E_N] \\ &= E_{N-1}(X_{\rm surf}) - E_{N-1}(X_{\rm bulk}),\end{aligned} \tag{40}$$

where N denotes the number of electrons in the system. The initial-state total energy E_N cancels due to the fact that there is only one initial state of the whole system,[6,25] whereby the shift becomes the difference between two final states. This raises the paradoxical question whether it is legitimate to speak of an initial-state contribution to the binding energy *shift*,[2] in spite of the intuitive notion that shifts in the core-electron *eigenvalues* ϵ_c would represent such a contribution. Within the framework of Hartree-Fock (HF) theory, Koopmans's theorem tells us that the HF orbital eigenvalue ϵ_c exactly equals the corresponding difference in total energy upon ionization

$$\epsilon_c = -(E^{\rm HF}_{N-1} - E^{\rm HF}_N), \tag{41}$$

where the $N-1$ electrons should remain frozen in their original distribution for the calculation of $E^{\rm HF}_{N-1}$. Hence the effects of electron relaxation, on the one hand, and electron correlation, on the other, are by no means incorporated in Eq. (41). Koopmans's theorem serves nevertheless as a formal, albeit approximate, connection between an orbital eigenvalue and its binding energy. However, as was strongly emphasized by Egelhoff,[2] but perhaps less clearly spelled out elsewhere in the literature, orbital eigenvalues in a multielectron system are mathematical constructions which satisfy the relation (41) but do not represent any *real* property of the initial or ground state of the system. The eigenvalue *probes* the initial state of the charge density and potential and gives an estimate of a total energy difference, which is the real representation of the binding energy.

The second approach used to associate an orbital eigenvalue with the inital-state contribution to a binding energy is to expand a total energy difference in a Taylor series.[23,2,1] A partial derivative of the total energy E with respect to core occupation n_c is within density functional formalism rigorously given by the corresponding eigenvalue ϵ_c. Directly applied to the middle expression in (40), i.e., using $\delta n_c = -1$, this gives[1,23]

$$\begin{aligned}\Delta_c = &-(\epsilon_c^{\rm surf} - \epsilon_c^{\rm bulk}) \\ &+\frac{1}{2}(\partial^2 E/\partial n^2_{c;\rm surf} - \partial^2 E/\partial n^2_{c;\rm bulk}) + \cdots\end{aligned} \tag{42}$$

or, explicitly separating the initial- and final-state contributions,[5,23]

$$\Delta_c = -\Delta\epsilon_c + \Delta E_{\rm rel}. \tag{43}$$

This expression represents the commonly used *identification* of the initial-state contribution with the core-eigenvalue shift and the labeling of the relaxation energy $\Delta E_{\rm rel}$ to effects that cannot be accounted for by the initial-state contribution.

The viewpoint that the origin of the SCLS is almost exclusively due to initial-state effects was expressed particularly strongly by Citrin and Wertheim.[5] The observed core-level shift for gold[8] was initially discussed in terms of s-d rehybridization at the surface and related to the observed shift of the valence d band.[8] Both the core-level shift and the surface d valence shift was then understood to be caused by a surface potential U, induced due to the narrowing of the surface-state density in conjunction with the approximate preservation of local charge neutrality.[21,22,5] In a model where the surface band is rigidly displaced by U for strict surface charge neutrality, a plausible connection between the initial and total contribution to the SCLS was provided by Desjonquères *et al.*[22]

$$\begin{aligned}\Delta_c(Z) \approx -\Delta\epsilon_c \cong -U(Z) &= \frac{\partial E_S(Z)}{\partial Z} \\ &\approx E_S(Z+1) - E_S(Z).\end{aligned} \tag{44}$$

Here, again, the final expression approximates the segregation energy in the sense that the impurity aspect has been neglected. From the aforementioned d-band charge neutrality model it immediately followed, i.e., completely within the initial-state concept, that for transition metals the SCLS (as connected to $\Delta\epsilon_c$ and U) should be of opposite sign for elements at the beginning and end of the series.[21,22] Moreover, the SCLS estimated by the model were found to be similar in magnitude to the measured shifts. Hence the trend in the SCLS across a transition series should most appropriately follow the eigenvalue shift $\Delta\epsilon_c$ implying that the final-state contribution $\Delta_{\rm rel}$ is rather small.[5]

In Table II we compare a number of core-eigenvalue shifts calculated previously with available experimental results. It may be seen that the value of this comparison is reduced by the fact that in the cases where several theoretical results refer to the same surface, there is a scatter of $\sim$0.2 eV. In Fig. 8 we therefore also make a comparison between the fcc(111) 1s-level shifts for the 4d metals obtained in the present full (1s core-hole) impurity calculations and the core-eigenvalue shifts extracted from a very recent study by Methfessel *et al.*[37] In this comparison we observe that the initial-state shifts are, on average, higher in energy than the screened total-energy results. A similar observation seems to hold for the net result of the comparison in Table II. The early results for Ta(100) and W(100) (Table II) led Johansson and Mårtensson[6] to suggest that the surface energy difference $E_S(Z+1) - E_S(Z)$ in Eq. (44) most naturally could be expanded around the hypothetical $(Z+\frac{1}{2})$ element. As a result, in the variation across a transition series in the initial-state shifts should be shifted systematically to

TABLE II. Comparison between independent first-principles calculatons (Calc.) of surface core-level eigenvalue shifts with experimenatal data (Expt.) for surface core-level binding energy shifts.

Metal	Surface	SCLS (eV) Calc.	Expt.
Ta	bcc (100)	0.96[a]	0.74[b]
W	bcc (110)		-0.32[c]
	bcc (100)	0.0[d]	-0.35[e]
Pt	fcc (111)		-0.40[f]
	fcc (100)	-0.87[g]	
	fcc (110)		-0.55[f]
Mo	bcc (110)	-0.14[h]	-0.33[i]
Ru	hcp (0001)	-0.5[j]	
Rh	fcc (111)	-0.46[k],-0.6[j]	
	fcc (100)	-0.59[h],-0.75[k],-0.75–0.81[l]	
Pd	fcc (100)	-0.30–0.41[l],-0.47[h], -0.55[m]	-0.44[n]

[a]Krakauer (Ref. 34).
[b]Guillot *et al.* (Ref. 12).
[c]Riffe *et al.* (Ref. 15).
[d]Posternak *et al.* (Ref. 29).
[e]van der Veen *et al.* (Ref. 10).
[f]Baetzold *et al.* (Ref. 11).
[g]Wang *et al.* (Ref. 35).
[h]Methfessel *et al.* (Ref. 37).
[i]Lundgren *et al.* (Ref. 19).
[j]Feibelman (Ref. 32).
[k]Feibelman and Hamann (Ref. 33).
[l]Arlinghaus *et al.* (Ref. 30).
[m]Kudrnovsky *et al.* (Ref. 55).
[n]Nyholm *et al.* (Ref. 20).

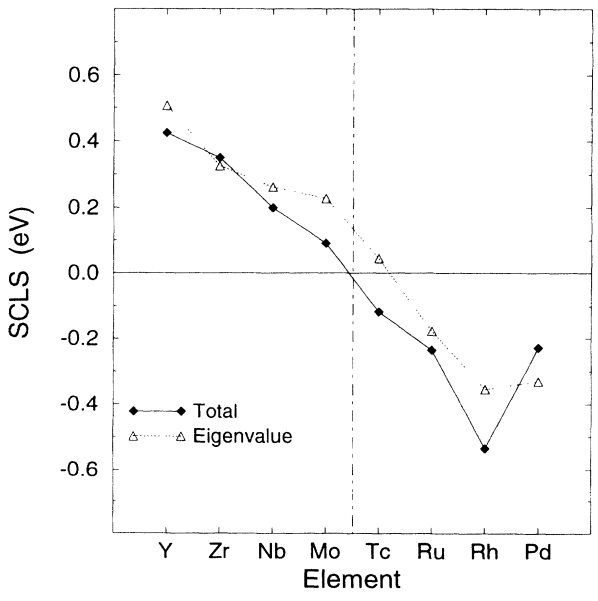

FIG. 8. Comparison of calculated 1*s*-level surface core-level shifts of the fcc(111) facet for the 4*d* metals, between those obtained within the present complete screening picture (solid diamonds, Total)and the corresponding core-eigenvalue shifts (open triangles, Eigenvalue) as reported by Methfessel *et al.* (Ref. 37). The vertical dashed line marks a half-filled *d* band (initial state).

the right of the original values by approximately half an element, which is strikingly close to what is seen in Fig. 8 for the sequence Nb-Pd. This picture has recently been supported by a tight-binding study[28] for closely packed bcc surfaces of Ta and W.

The remaining problem that needs to be understood is the fact that two completely different physical interpretations serve to give similar shifts. The initial-state core-eigenvalue shifts are indeed close in magnitude to the shifts obtained by the present type of impurity calculations, where the shift may unambiguously be traced to the screening properties of the valence *d* electrons. If there was a contribution due to the core-eigenvalue shift, one could for a moment argue that the screening contribution would itself enhance the shift by a factor of ~2.

It should be stressed that the screened SCLS presented above and in Sec. III were obtained by means of the frozen-core approximation. Hence the shift is identified solely with the difference in the total energy[40,46] associated with the valence charge. To the extent that such a scheme is a good approximation to a full treatment, it indicates that differences in the core eigenvalues for a bulk and surface atom, respectively, have indeed only a minor *real* effect on the observed SCLS. For a perturbed system, e.g., a surface, a change δv in the one-electron potential shifts the core-electron eigenvalues ϵ_i by

$$\delta\epsilon_i = \int \delta v |\psi_i|^2 d^3r \tag{45}$$

under the constraint, as in the frozen-core approximation, that the core orbitals ψ_i are kept frozen. The core contribution to the total energy may be identified with the kinetic energy part

$$T_{\text{core}}^{\text{kin}} = \sum_i \epsilon_i - \int_r v n_{\text{core}} d^3r, \tag{46}$$

where the sum runs over the core states and n_{core} is the core charge density. The change in this contribution upon the shift δv, using $n_{\text{core}}=\sum_i |\psi_i|^2$, is

$$\delta T_{\text{core}}^{\text{kin}} = \sum_i \delta\epsilon_i - \int \delta v n_{\text{core}} d^3r = 0, \tag{47}$$

whereby the effect of a core-eigenvalue shift will be completely cancelled in the total energy differences, e.g., those used for the segregation energy calculation. This result is of course modified if the core orbitals are allowed to relax, and the validity of the frozen-core approximation has been examined by von Barth and Gelatt.[77] The essential result is that the error in the total energy due to this approximation vanishes to first order in the charge density differences, becoming typically 2% of the total energy of transformation between two different chemical environments.

It is completely evident that, for transition metals at least, the calculated core-eigenvalue shifts are indeed similar to the experimentally observed SCLS. On the other hand, it may be argued on the basis of the above discussion that the former quantity has no direct relevance for the latter and that the observed qualitative agreement

therefore appears to be fortuitous.

To elucidate the origin of the agreement between the core-eigenvalue shifts and the measured SCLS, we shall consider the screening properties of the d electrons. The one-electron contribution from the d states to the bonding energy for a system with n d electrons may be written

$$E^{\text{one-el}}(n) = \int^{\epsilon_F} (\varepsilon - C_n) D(\varepsilon) d\varepsilon, \tag{48}$$

where ϵ_F is the Fermi level (defined to be fixed for the present purposes) , C is the d-band centroid, and D is the d state density. For a model with a rigid state density, neglecting the impurity aspect and charge transfer, the corresponding energy of the screened core hole is therefore given by

$$E^{\text{one-el}}(n+\delta n) = \int^{\epsilon_F} (\varepsilon - C_{n+\delta n}) D(\varepsilon + \delta t) d\varepsilon, \tag{49}$$

where δn is the screening d charge and δt is the amount by which the d states are pulled down relative to ϵ_F. Hence the screening energy may be written

$$\begin{aligned} \Delta E^{\text{one-el}}_{\delta n} &= E^{\text{one-el}}(n+\delta n) - E^{\text{one-el}}(n) \\ &= \int_{\epsilon_F}^{\epsilon_F+\delta t} \varepsilon D(\varepsilon) d\varepsilon - (n+\delta n)(\delta t + C_{n+\delta n}) \\ &\quad + n C_n, \end{aligned} \tag{50}$$

where we have used $n = \int^{\epsilon_F} D(\varepsilon) d\varepsilon$. Expanding C_n and $C_{n+\delta n}$ around $n + \delta n/2$, e.g., $C_n \cong C_{n+\delta n/2} + \delta t/2$, and the integrand around $\epsilon_F + \delta t/2$, we obtain

$$\frac{\Delta E^{\text{one-el}}_{\delta n}}{\delta n} \cong \epsilon_F - C_{n+\delta n/2}. \tag{51}$$

The analysis applies equally well to bulk and surface atoms. Since $\delta n \cong 1$ for both bulk and surface screening, the SCLS becomes the difference between the bulk (B) and surface (S) d-band centers for a hypothetical d valence of $n + \delta n/2$, i.e.,

$$\Delta_c \approx -(C^S_{n+\delta n/2} - C^B_{n+\delta n/2}). \tag{52}$$

This result should be compared with the estimate of the core-eigenvalue shift,[5,21,22,28]

$$\Delta\epsilon_c \approx -(C^S_n - C^B_n), \tag{53}$$

which suggests that an "initial-state" shift for the Z element should be interpreted as the "total" shift for the hypothetical $(Z-1/2)$ element.[6] This is essentially Slater's transition state. The result (53) and (52) may of course also be regarded as an alternative formulation of Eq. (44).

It follows from the analysis that both the core-eigenvalue shift and the "total energy" shift may be described in terms of the shift in the band centroid, although translated by half an element. The band shift is electrostatically induced, governed by surface band narrowing in conjunction with conservation of d charge when proceeding from the bulk to the surface. We have thus clarified the effect of this physical condition, namely, that it is simultaneously responsible for (a) the screening properties, which is directly related to the SCLS, and (b) the core-eigenvalue shift, which probes the initial state, but is otherwise irrelevant for the SCLS.

B. The impurity contribution

The thermodynamical formulation (30) in Sec. II E expressed the SCLS as the difference between two surface energies plus a term which is commonly referred to as the impurity contribution. In the computational procedures this clear-cut separation into surface energy and impurity contribution to the shift is not carried out explicitly. It has nevertheless become customary, and physically convenient, to discuss the origin of the shift in terms of these contributions. If one uses the equivalent-core approximation and neglects the impurity terms in (30) the SCLS may *essentially* be interpreted as the difference between the surface energy of the $(Z+1)$ and Z elements, which is usually thought of as the most important contribution. It was therefore proposed[14] that the anomalously high SCLS of Re(0001) was due to the differences in the Z dependence of the surface energy induced by the crystal structure. This picture is confirmed by the surface energy results of Skriver and Rosengaard[48] and by the fact that in the present calculations we find that for the bcc(110) face the surface energy maximum occurs at W while for the hcp(0001) face the maximum is found at Os.

To obtain a qualitative measure of the importance of the impurity aspect relative to the surface energy, we may use our calculated surface energies to estimate the SCLS from $E_S^{Z+1} - E_S^Z$ as a function of atomic volume and crystal structure. A comparison between the calculated SCLS of the fcc(111) face of the $5d$ metals from Table I

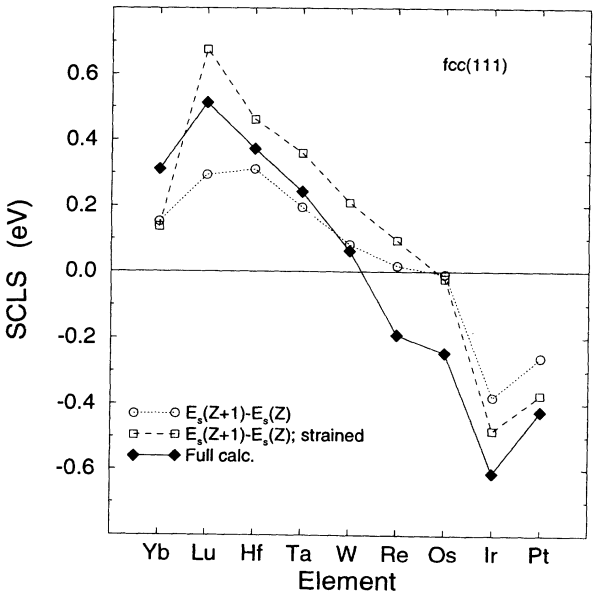

FIG. 9. Comparison for fcc(111) between calculated surface core-level shifts (solid diamonds) and estimates using $E_S^{Z+1} - E_S^Z$ (Z is the atomic number). Circles, surface energies E_S were obtained for the natural (experimental) volume of each element Z; squares (strained), E_S^{Z+1} and E_S^Z both calculated for the atomic volume of the Z metal.

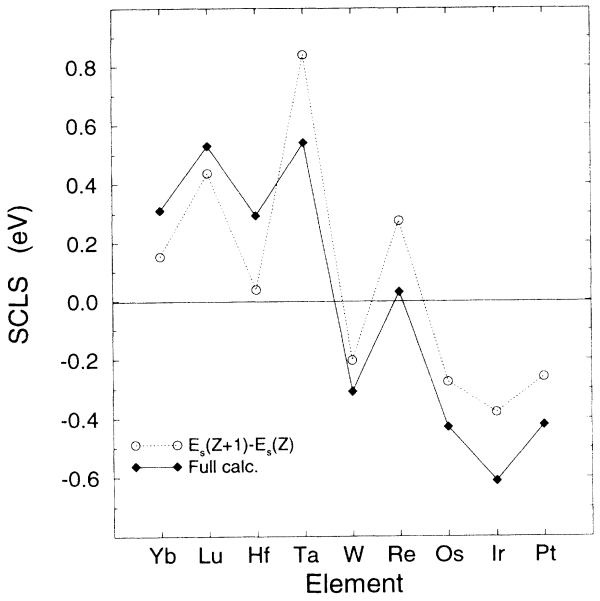

FIG. 10. Comparison between calculated surface core-level shifts for the most closely packed surface of the observed crystal structures (solid diamonds) and estimates using $E_S^{Z+1} - E_S^Z$ (open circles). Here E_S^{Z+1} and E_S^Z were both calculated in the observed crystal structure of the Z metal, but for the different (nonstrained) volumes of the $(Z+1)$ and Z elements, respectively.

and two different $E_S^{Z+1} - E_S^Z$ estimates is presented in Fig. 9. If E_S^{Z+1} is calculated at the atomic volume of the (Z+1) metal, i.e., simulating a "nonstrained" final state, the SCLS is typically underestimated for the earlier elements (where the volume differences are large) relative to the more realistically "strained" situation. The difference between these two situations may thus serve as a qualitative measure of the strain energy in the final state.

Turning to the dependence on crystal structure, we show in Fig. 10 estimates of $E_S^{Z+1} - E_S^Z$ obtained by "nonstrained" surface energies where both E_S^{Z+1} and E_S^Z are calculated in the observed structure of the Z metal. Now the anomaly close to W and Re appear qualitatively correct, indicating that this behavior is indeed connected with the crystal dependence of the surface energy. It is also clear that the difference in SCLS between a metal in the fcc and the hcp structure may be substantial, i.e., already from the calculated surface energies, in spite of the fact that the two structures have the same coordination number.

It appears that the present calculations confirm the picture[6] that for transition metals the so-called surface-energy contribution provide the dominant features over the series, although the impurity contribution, here of the order of 0.2 eV, is still important and cannot be neglected in quantitative studies. One should, however, remember the ambiguity caused by the slightly different definitions of the impurity terms as discussed in Sec. II E.

The SCLS peaks observed in bcc W and hcp Re will in fact also appear if the surface energy E_S is related to the cohesive energy $E_{\rm coh}$ by the familiar approximate relation $E_S \approx 0.2E_{\rm coh}$.[6] Equation (29) then becomes

$$\Delta_c \approx 0.2(E_{\rm coh}^{Z+1} - E_{\rm coh}^Z) - 0.2E_{{\rm imp}(Z+1)}^{\rm bulk}, \qquad (54)$$

where we have used that $E_{{\rm imp}(Z+1)}^{\rm surface} \approx 0.8E_{{\rm imp}(Z+1)}^{\rm bulk}$. However, as pointed out in Ref. 14, the irregularities are then of atomic origin and will not appear if one uses cohesive energies related to the same type of $d^n s^1$ multiplet average atomic state for all the $5d$ elements.[14]

V. SUMMARY

We have implemented an efficient matrix Green's-function technique for calculating the electronic structure of an impurity located in the bulk or at the surface. The technique is based on the generalized linear-muffin-tin-orbitals method and a Green's-function formalism. For the charge density we apply the frozen-core and atomic-sphere approximations, but, in addition, we include the contribution from the charge density dipoles in the inter-sphere potentials. We have taken great care to maintain identical approximations and computational parameters in the bulk and at the surface thus keeping the numerical errors in the calculated segregation energies at a minimum.

We have used the Green's-function technique in a comprehensive theoretical study of the surface core-level shifts of the $4d$ and $5d$ transition metals. We have included the so-called final-state effects by identifying the shift with the surface segregation energy of a core-ionized impurity. In those cases where the measured data are obtained from single crystals, our results are in good agreement with experiment. This gives quantitative support to the complete screening picture of the core-electron photoionization process. We also conclude that the frozen-core and atomic-sphere approximations are well justified for closely packed surfaces, which indeed helps to isolate and clarify the main contribution to the SCLS. Finally, the calculations of the SCLS for several crystal structures provide a better understanding of the observed changes across a d transition series.

ACKNOWLEDGMENTS

M.A., I.A.A., and B.J. are grateful to The Göran Gustafsson Foundation and The Swedish Natural Science Research Council for financial support. The Center for Atomic-Scale Materials Physics is sponsored by the Danish National Research Foundation. Part of the work was supported by grants from the Novo Nordisk Foundation and the Danish research councils through the Danish Center for Surface Reactivity.

[1] D. Spanjaard, C. Guillot, M.C. Desjonquères, G. Tréglia, and J. Lecante, Surf. Sci. Rep. **5**, 1 (1985).
[2] W.F. Egelhoff, Surf. Sci. Rep. **6**, 253 (1987).
[3] N. Mårtensson, A. Stenborg, D. Björneholm, A. Nilsson, and J.N. Andersen, Phys. Rev. Lett. **60**, 1731 (1988).
[4] B. Johansson and N. Mårtensson, Phys. Rev. B **21**, 4427 (1980).
[5] P.H. Citrin and G.K. Wertheim, Phys. Rev. B **27**, 3176

(1983).
[6] B. Johansson and N. Mårtensson, Helv. Phys. Acta **56**, 405 (1983).
[7] H. Tillborg, Ph.D. thesis, Uppsala University, 1993.
[8] P.H. Citrin, G.K. Wertheim, and Y. Baer, Phys. Rev. Lett. **41**, 1425 (1978).
[9] J.F. van der Veen, P. Heimann, F.J. Himpsel, and D.E. Eastman, Solid State Commun. **37**, 555 (1981).
[10] J.F. van der Veen, P. Heimann, F.J. Himpsel, and D.E. Eastman, Solid State Commun. **38**, 595 (1981).
[11] R.C. Baetzold, G. Apai, and E. Shustorovich, Phys. Rev. B **26**, 4022 (1982).
[12] C. Guillot, D. Chauveau, P. Roubin, J. Lecante, M.C. Desjonquères, G. Tréglia, and D. Spanjaard, Surf. Sci. **162**, 46 (1985).
[13] S.D. Barrett, A.M. Begley, P.J. Durham, and R.G. Jordan, Solid State Commun. **71**, 111 (1989).
[14] N. Mårtensson, H.B. Saalfeld, H. Kuhlenbeck, and M. Neumann, Phys. Rev. B **39**, 8181 (1989).
[15] D.M. Riffe, G.K. Wertheim, and P.H. Citrin, Phys. Rev. Lett. **63**, 1976 (1989).
[16] D.M. Riffe and G.K. Wertheim, Phys. Rev. B **47**, 6672 (1993).
[17] A. Flodström, R. Nyholm, and B. Johansson, in *Advances in Surface and Interface Science, Volume 1: Techniques*, edited by R.Z. Bachrach (Plenum Press, New York, 1992).
[18] N. Mårtensson (private communication); A. Stenborg, Ph.D. thesis, Uppsala University, 1989.
[19] E. Lundgren, U. Johansson, M. Qvarford, J.N. Andersen, and R. Nyholm, in *MAX-LAB Activity Report 1991*, edited by U.O. Karlsson and S.L. Sorensen (KF-Sigma, Lund, 1991); E. Lundgren, U. Johansson, R. Nyholm, and J.N. Andersen, Phys. Rev. B **48**, 5525 (1993).
[20] R. Nyholm, M. Qvarford, J.N. Andersen, S.L. Sorensen, and C. Wigren, J. Phys. Condens. Matter. **4**, 277 (1992).
[21] P.J. Feibelman and D.R. Hamann, Solid State Commun. **31**, 413 (1979).
[22] M.C. Desjonquères, D. Spanjaard, Y. Lassailly, and C. Guillot, Solid State Commun. **34**, 807 (1980).
[23] A.R. Williams and N.D. Lang, Phys. Rev. Lett. **40**, 954 (1978).
[24] A. Rosengren and B. Johansson, Phys. Rev. B **23**, 3852 (1981).
[25] W.F. Egelhoff, Phys. Rev. Lett. **50**, 587 (1983).
[26] A. Rosengren and B. Johansson, Phys. Rev. B **22**, 3706 (1980).
[27] A. Rosengren, Phys. Rev. B **24**, 7393 (1981).
[28] M. Said, M.C. Desjonquères, and D. Spanjaard, Phys. Rev. B **47**, 4722 (1993).
[29] W(100): M. Posternak, H. Krakauer, A.J. Freeman, and D.D. Koelling, Phys. Rev. B **21**, 5601 (1980); E. Wimmer, A.J. Freeman, J.R. Hiskes, and A.M. Karo, *ibid.* **30**, 6834 (1983).
[30] Rh(100) and Pd(100): F.J. Arlinghaus, J.G. Gay, and J.R. Smith, Phys. Rev. B **23**, 5152 (1981).
[31] J.R. Smith, F.J. Arlinghaus, and J.G. Gay, Phys. Rev. B **26**, 1071 (1982).
[32] Ru(0001): P.J. Feibelman, Phys. Rev. B **26**, 5347 (1982).
[33] Rh(111) and Rh(100): P.J. Feibelman and D.R. Hamann, Phys. Rev. B **28**, 3092 (1983).
[34] Ta(100): H. Krakauer, Phys. Rev. B **30**, 6834 (1984).
[35] Pt(100): D.-S. Wang, A.J. Freeman, and H. Krakauer, Phys. Rev. B **29**, 1665 (1984).
[36] A.M. Begley, R.G. Jordan, W.M. Temmerman, and P.J. Durham, Phys. Rev. B **41**, 11 780 (1990).
[37] M. Methfessel, D. Hennig, and M. Scheffler, Surf. Sci. **287/288**, 785 (1993).
[38] P.J. Feibelman, Phys. Rev. B **39**, 4866 (1989).
[39] O. K. Andersen, Phys. Rev. B **12**, 3060 (1975)
[40] O. Gunnarsson, O. Jepsen, and O.K. Andersen, Phys. Rev. B **27**, 7144 (1983).
[41] H.L. Skriver, *The LMTO Method* (Springer, Berlin, 1984).
[42] O.K. Andersen and O. Jepsen, Phys. Rev. Lett. **53**, 2571 (1984)
[43] O.K. Andersen, O. Jepsen, and D. Glötzel, in *Highlights of Condensed-Matter Theory*, edited by F. Bassani, F. Fumi, and M. P. Tosi (North-Holland, New York, 1985).
[44] O.K. Andersen, Z. Pawlowska, and O. Jepsen, Phys. Rev. B **34**, 5253 (1986).
[45] W.R.L. Lambrecht and O. K. Andersen, Surf. Sci. **178**, 256 (1986), and private communication.
[46] H.L. Skriver and N.M. Rosengaard, Phys. Rev. B **43**, 9538 (1991).
[47] H.L. Skriver and N.M. Rosengaard, Phys. Rev. B **45**, 9410 (1992).
[48] H.L. Skriver and N.M. Rosengaard, Phys. Rev. B **46**, 7157 (1992).
[49] M. Aldén, H.L. Skriver, S. Mirbt, and B. Johansson, Phys. Rev. Lett. **69**, 2296 (1992).
[50] M. Aldén, S. Mirbt, H.L. Skriver, N.M. Rosengaard, and B. Johansson, Phys. Rev. B **46**, 6303 (1992).
[51] S. Mirbt, H.L. Skriver, M. Aldén, and B. Johansson, Solid State Commun. **88**, 331 (1993).
[52] N.M. Rosengaard and H.L. Skriver, Phys. Rev. B **47**, 12 865 (1993).
[53] I.A. Abrikosov and H.L. Skriver, Phys. Rev. B **47**, 16 532 (1993).
[54] A.V. Ruban, I.A. Abrikosov, D.Ya. Kats, D. Gorelikov, K.W. Jacobsen, and H.L. Skriver, Phys. Rev. B **49**, 11 383 (1994).
[55] J. Kudrnovsky, I. Turek, V. Drchal, P. Weinberger, N.E. Christensen, and S. K. Bose, Phys. Rev. B **46**, 4222 (1992).
[56] J. Kudrnovsky, I. Turek, V. Drchal, P. Weinberger, S.K. Bose, and A. Pasturel, Phys. Rev. B **47**, 16 525 (1993).
[57] M. Methfessel, D. Hennig, and M. Scheffler, Phys. Rev. B **46**, 4816 (1992).
[58] R. Poudloucky, R. Zeller, and P.H. Dederichs, Phys. Rev. B **22**, 1577 (1980).
[59] P. J. Braspenning, R. Zeller, A. Lodder, and P. H. Dederichs, Phys. Rev. B **29**, 703 (1984).
[60] B. Drittler, M. Weinert, R. Zeller, and P. H. Dederichs, Phys. Rev. B **39**, 930 (1989).
[61] U. Klemradt, B. Drittler, R. Zeller, and P. H. Dederichs, Phys. Rev. Lett. **64**, 2803 (1990).
[62] C. Koenig, N. Stefanou, and J. M. Koch, Phys. Rev. B **33**, 5307 (1986).
[63] P.J. Feibelman, Phys. Rev. B **35**, 2626 (1987).
[64] M. Scheffler, C. Droste, A. Fleszar, F. Máca, G. Wachutka, and G. Barzel, Physica B **172**, 143 (1991).
[65] G. Wachutka, A. Fleszar, F. Máca, and M. Scheffler, J. Phys. Condens. Matter **4**, 2831 (1992).
[66] A. Gonis, G. M. Stocks, W. H. Butler, and H. Winter, Phys. Rev. B **29**, 555 (1984).
[67] J. C. Slater, *Quantum Theory of Molecules and Solids* (McGraw-Hill, New York, 1963), Vol. 1.

[68] C.J. Bradley and A.P. Cracknell, *The Mathematical Theory of Symmetry in Solids* (Clarendon Press, Oxford, 1972).
[69] G. Ries and H. Winter, J. Phys. F **9**, 1589 (1979).
[70] B. Wenzien, J. Kudrnovskỳ, V. Drachal, and M. Sob, J. Phys. Condens. Matter **1**, 9893 (1989).
[71] For the present application of a "$(Z+1)$ impurity" in a Z metal host, the phase shift resides between 0 and π.
[72] S.H. Vosko, L. Wilk, and M. Nusair, Can. J. Phys. **58**, 1200 (1980).
[73] J. Friedel, Ann. Phys. (Paris) **1**, 257 (1976).
[74] E. Navas, K. Starke, C. Laubschat, E. Weschke, and G. Kaindl, Phys. Rev. B **48**, 14 753 (1993); A.V. Fedorov, E. Arenholz, K. Starke, E. Navas, L. Baumgarten, C. Laubschat, and G. Kaindl (unpublished).
[75] R. Manne and T. Åberg, Chem. Phys. Lett. **7**, 282 (1970).
[76] G. Crecelius, G.K. Wertheim, and D.N.E. Buchanan, Phys. Rev. B **18**, 6519 (1978).
[77] U. von Barth and C.D. Gelatt, Phys. Rev. B **21**, 2222 (1980).